GIS-based Bivariate Analysis of the Impact of Climate on the Abu Dhabi (UAE) Mangrove National Park

Asif Raihan[1], Tarig Ali[2], Md. Maruf Mortula[3]

[1] Department of Civil Engineering, Eastern University, Dhaka, Bangladesh – b00089588@alumni.aus.edu
[2] Department of Civil Engineering, American University of Sharjah, United Arab Emirates – atarig@aus.edu
[3] Department of Civil Engineering, American University of Sharjah, United Arab Emirates – mmortula@aus.edu

Keywords: Land Surface Temperature, Normalized Difference Vegetation Index, Environment, Climate Change, Landsat 8

Abstract

Mangrove is a vital natural resource, satisfying the various demands of both humans and other aquatic habitats. Also, it shields against natural disasters. Extensive researches were conducted on the benefits of mangrove to combat climate change. But limited works were done to assess the impact of microclimate factors on mangrove. This study examined the impact of climate represented by Land Surface Temperature on mangrove forest health (i.e., Normalized Difference Vegetation Index) for Abu Dhabi Mangrove National Park, covering the period: 2015-2020. To accomplish this, Local Bivariate Analysis was performed. Firstly, satellite images from Landsat 8 covering the study area were downloaded and pre-processed. Then, values of the variables were computed, extracted as points and then analysed. Results showed that the mangrove exhibited different temperature and vegetation health relationships (i.e., Positive Linear, Negative Linear, Concave, Convex, Not Significant, etc.). Also, results showed that mangrove health has degraded due to surface temperature increase. Furthermore, the coefficient of determinations of the bivariate analysis of the mangrove and the land surface temperature in 2020 is higher compared to that of 2015 with the highest $R^2 = 0.8512$ (Convex) followed by $R^2 = 0.8192$ (Concave) and $R^2 = 0.7281$ (Negative Linear).

1. Introduction

Mangroves dominate a significant portion of the Earth's cover, providing coastal inhabitants with protection from a number of natural calamities (Rostami et al., 2022), (Morris et al., 2023), (Liu et al., 2022). Furthermore, mangroves provide consumable resources for both aquatic creatures and humans (Malik et al., 2017). Despite their resiliency against both natural and anthropogenic factors, mangroves perish globally as seen by the presence of their peat deposits (Alongi, 2015).

The mangrove ecosystem in the UAE is located in two different areas: Abu Dhabi and Northern UAE. In Abu Dhabi, mangrove spreads over 70 km^2 with the Mangrove National Park spreads one third of the area (T.S., 2014). The mangroves in the Northern UAE are located in Ajman's Creek, Dubai Creek, Khor Fakkan, Umm Al Quwain Hamriyah's Creek, and Ras Al Khaimah. The average tree height in these areas is 2.5m (Moore et al., n.d.). The soil compositions in these zones are porous loamy silt and clay, retaining seawater for an extended period (Bashitialshaaer et al., 2011). Generally, positive contributions of mangroves to stabilize climate change have been broadly covered, but factors affecting mangrove ecosystem are yet to be fully explored. Such one factor is Land Surface Temperature (LST).

LST is one of the crucial parameters, affecting the growth and development of mangroves. Remote sensing is an excellent option to detect LST changes for coastal areas. For instance, at the coastal Kanyakumari district of India, LST was determined using MODIS (Moderate Resolution Imaging Spectroradiometer) satellite images to find that salt pan had high temperature (i.e., 31.57 ◦C). Whereas, waterbodies exuded low LST (28.9 ◦C) (Sam & Balasubramanian, 2023). Recently, several attempts have been made to establish a relationship between LST and mangrove NDVI. A weak but statistically significant negative relationship governing LST with respect to mangrove NDVI revealed that decrease in mangrove forests could end up increasing the LST of Sundarbans mangrove forest in Bangladesh and India (Kanjin & Alam, 2024). Although, with a weak correlation between LST and NDVI for mangroves, high mangrove health was yielded under a specific temperature window (i.e., 30-33 ◦C) for UAE mangrove system during summertime (Raihan et al., 2023). A further study on the relationship between UAE mangroves' health with LST stated LST-NDVI relationship to be complex when spatial and temporal correlations were separately accounted. But the inclusion of several machine learning algorithms coupled merging both spatial and temporal aspects showcased highest mangrove biomass in the temperature range 30-35 ◦C (Raihan et al., 2024).

Mangrove restoration practice is also affected by climate change. One study pointed that the presence of high temperature with eutrophication caused mangrove seedlings to have low root growth with long stems, resulting in structural imbalance to the plants which made them vulnerable to external forces by easily uprooting them (Cobacho et al., 2024). Manmade activities play a key role in degrading mangrove forest covers with increase in LST. An investigation on the effect of NDVI on LST along the southern Sumatra coast of Indonesia revealed that areas with temperature >20 ◦C were accompanied with mangrove loss. Also, there was a moderate correlation between LST and NDVI ($r = 0.74$, $p < 0.05$). Also, built-up index greatly influenced vegetation cover area at the study site (Rendana et al., 2023).

Trend analysis between temperature variation and mangrove extents seems to be promising. Such endeavor was conducted in the mangrove located at southern Iran. It was found that mangrove extent was increased from 73.08 km^2 to 88.73 km^2 (by 21%) between 1981 and 2017. Although the mean temperature did not show a significant trend during the study period but minimum temperature exhibited highest correlation with mangrove forest extent (i.e., 61%) (Rostami et al., 2022). Another work involved assessing spatio-temporal changes in LST over South Asia. Central and southwest Asia demonstrated

This contribution has been peer-reviewed. The double-blind peer-review was conducted on the basis of the full paper.
https://doi.org/10.5194/isprs-annals-X-G-2025-681-2025 | © Author(s) 2025. CC BY 4.0 License.

highest daytime cooling in December as opposed to nighttime warming in central and northwest in July and September. Under the research, nineteen ecoregions experienced monthly daytime cooling. However, one region called “Indus River Delta-Arabian Sea mangroves” had monthly and annual nighttime warming magnitude at annual scale (i.e., 0.06 ◦C/yr at 99% Confidence Level) (Shawky et al., 2023). Global mangrove NDVI variations in both spatial and temporal aspects were assessed using satellite and remote sensing techniques between 2000 and 2018. It was found that average mangrove NDVI of the Asian region was the highest (0.80). Whereas, the mean mangrove NDVI at African zones was the lowest (0.67). Also, global mangrove NDVI demonstrated positive correlation with temperature (R_{temp} = 0.37, p value < 0.01) (Ruan et al., 2022).

Some past researches also covered leaf damage of mangroves due to extreme low temperature (Chen et al., 2017), (Osland et al., 2017), (Lovelock et al., 2016). High temperature could also negatively affect mangroves due to elevated respiration and lowered photosynthesis (Lovelock et al., 2016). Temperature in conjunction with additional climatic factors played a key part in maximum mangrove canopy heights, distribution and biomass and this phenomenon varied spatially (Simard et al., 2019). Microclimate changes due to temperature variation (i.e., 2◦C to 14 ◦C) resulted in mangrove damage to winter temperature (Wu et al., 2018). Furthermore, LST variations could hamper mangrove expansion in some zones but facilitated mangrove growth in other areas (Osland et al., 2019).

By referring to the previous studies, it is discerned that for determining LST at coastal areas, most of the works centered towards utilizing MODIS satellite images. Also, focus was given on the effect(s) of mangrove vegetation health on LST by figuring out weak yet statistically significant relationships between the two parameters. Also, the combined impact of LST with some man-made factors influencing mangrove NDVI was highlighted. Furthermore, general trend analyses were performed to represent both LST and NDVI variations over a period of time at a specific region of interest. Few studies considered the effect(s) of extreme low and high temperatures on mangrove health along with their associated influence with other microclimate parameters. To the best of our understanding, no study exhaustively covered the effect of LST on mangrove NDVI for the coastal areas of UAE by means of GIS and remote Sensing with the application of Local Bivariate Analysis (LBA). LBA could help explain in further details the local influence on the alterations of LST-NDVI associations over a time period. Also, LBA would cover the complexities of the relationship which would expand on the simple linear regression for LST-NDVI aspect. Therefore, the objective of this paper is to derive the relationship between LST and NDVI by the means of the aforesaid techniques for UAE mangrove ecosystem over the period: 2015-2020.

2. Materials and Methods

This research endeavour encompassed Abu Dhabi mangrove national park of UAE. The primary steps to accomplish pre and postprocessing of the work are provided below (Figure 1):

- Sample mangrove site selection (i.e., Abu Dhabi Mangrove National Park).
- Pre-processing of the Landsat images: this process includes radiometric corrections, band-stacking, mosaicking for the raster layers, conversion of Geographic Coordinate System (GCS) to unified projected coordinate system (PCS).
- Further methods used to study the impact of LST on mangrove NDVI.

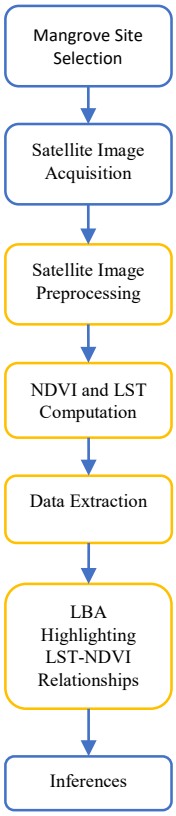

Figure 1. Flow chart depicting the main processes

2.1 Sites selection and Acquisition

Abu Dhabi Mangrove National Park (54.4230091°E 24.4561825°N) was selected based on its importance, relevance, size, etc. This site was specially considered for its potentiality to extract relevant climate data for local bivariate evaluation (Figure 2).

Figure 2. Locator map for Abu Dhabi Mangrove National Park

This contribution has been peer-reviewed. The double-blind peer-review was conducted on the basis of the full paper.
https://doi.org/10.5194/isprs-annals-X-G-2025-681-2025 | © Author(s) 2025. CC BY 4.0 License.

Landsat Images for the years 2015, and 2020 covering the mangrove site were acquired from the USGS (United States Geological Survey) (*USGS Earth Explorer*, n.d.). For deriving the climate factors, all of the images were acquired between the summertime (i.e., June-July) with less than 10% cloud cover to eliminate atmospheric interferences and maintain consistency.

Satellite images for 2015 and 2020 were obtained from Landsat 8. It carried OLI (Operational Land Imager) and TIRS (Thermal Infrared Sensors) devices. Only the image paths and rows that aligned with Abu Dhabi Mangrove National Park were chosen (i.e., 160 043 and 161 043).

2.2 Satellite image preprocessing

Landsat images were radiometrically corrected to eliminate atmospheric interference resulting from absorption, scattering, etc. of solar radiation by clouds and other airborne particles to extract refined information obtained from the images to perform accurate quantitative analysis. This process involved the conversion of raw Digital Numbers (DNs) of satellite images to radiance and ultimately reflectance. At first, DN values were converted to radiance which is the energy flux (i.e., irradiant/incident energy) per solid angle leaving a unit surface area in a given direction. To accomplish this, a series of gains and biases obtained from the metadata of the satellite images was used.

$$L_\lambda = M_L * Q_{cal} + A_L \quad (1)$$

Where L_λ= Spectral radiance at sensor's aperture ($\frac{watts}{m^2 ster \mu m}$)
M_L= Band specific multiplicative rescaling factor from Landsat image metadata file
A_L = Band-specific additive rescaling factor from Landsat metadata file
Q_{cal} = Quantized and calibrated standard product pixel value (DN)

Radiance is depended upon illumination, orientation and position of a target feature(s) along with the light's path through atmosphere (which is further influenced by absorption and scattering). Therefore, radiance introduces some variabilities in measurements. To rectify this, spectral radiance was converted into Top of Atmosphere (TOA) reflectance, resulting in atmospheric influence removal with reliable measurements. Reflectance is the proportion of solar radiation striking a point to the radiation reflected from it (Parks, 2020).

$$\rho_p = \frac{\pi * L_\lambda * d^2}{ESUN_\lambda * cos\theta_s} \quad (2)$$

Where ρ_p= TOA reflectance (unit less ratio of the reflected solar energy to incident solar energy)
L_λ= Spectral radiance at sensor's aperture
d= Earth-Sun distance in astronomical units (provided in the image metadata file)
$ESUN_\lambda$= Mean Solar exo-atmospheric irradiances ($\frac{w}{m^2 \mu m}$)

After the preprocessing, Landsat images for each considered year were band stacked in order of the band numbers so that different band combinations could be applied to the color gun of the software to effectively visualize and further analyze different features found in the image along with making the images vibrant.

Then, the band stacks for a specific year were mosaicked to form a whole image covering the desired area. Prior to mosaicking, all the images were re-projected into a common Projected Coordinate System (PCS), which is the WGS 1984 UTM Zone 40N.

2.3 Mangrove NDVI computation

NDVI is one of the spectral indices, commonly used to examine the density, health and extent of mangrove vegetation. It is derived from the ratio of NIR and Red bands as shown in equation 5 below (Siddan & C.R., 2016):

$$NDVI = \frac{NIR - Red}{NIR + Red} \quad (3)$$

For Landsat 5 and Landsat 7 satellite images, bands 3 and 4 are red and near infrared. For Landsat 8, bands 4 and 5 are red and NIR respectively. NDVI is favoured compared to other indices as it is reported to have high accuracy in mangrove mapping. In addition, its computation is simple (Akbar et al., 2020). Furthermore, in one specific study, mangrove vegetation density was accurately assessed by computing NDVI relative to 23 other indices (Muhsoni et al., 2018).

2.4 LST computation

For Landsat 8, LST was computed using band 10 (Thermal Infrared) with 100 m spatial resolution. Top of atmospheric spectral radiance was computed from band 10, followed by conversion of radiance to at-sensor temperature. After that, NDVI method was applied for emissivity correction. Finally, LST was computed from land surface emissivity (Avdan & Jovanovska, 2016).

$$T = \frac{K_2}{ln\left(\frac{K_1}{L_\lambda} + 1\right)} \quad (4)$$

Where T = Effective at-sensor brightness temperature
K_2= Calibration constant 2 (k)
K_1= Calibration constant 1($\frac{watts}{m^2 ster \mu m}$)
L_λ= Spectral radiance at sensor's aperture ($\frac{watts}{m^2 ster \mu m}$)

Then, the brightness temperature (i.e., surface temperature in kelvin) was converted into degree Celsius (Siddan & C.R., 2016).
Finally, brightness temperature (T) was converted to LST by also considering emissivity (ϵ).

$$LST = \frac{T}{1 + \left(0.00115 * \frac{T}{1.4388}\right) * ln(\epsilon)} \quad (5)$$

For Landsat 8, thermal band 10 was used for LST to avoid large calibration uncertainty in thermal band 11. This is because, one study proposed that there was a negligible difference in LSTs when Landsat 8 band 10 was compared with Landsat 7 ETM+ thermal band when it came to vegetation cover. Whereas, a noticeable difference in surface temperature reading was obtained when Landsat 8 thermal band 11 was chosen against Landsat 7 ETM+ band 6 (Xu & Huang, 2016).

2.5 LST and NDVI samples extraction from satellite images

To study the relationship of LST with mangrove health (i.e., NDVI) on a local scale, Abu Dhabi Mangrove National Park (Number of samples = 136) in the UAE were considered. Then,

This contribution has been peer-reviewed. The double-blind peer-review was conducted on the basis of the full paper.
https://doi.org/10.5194/isprs-annals-X-G-2025-681-2025 | © Author(s) 2025. CC BY 4.0 License.

point feature was created and sample representations of both the aforementioned parameters (i.e., LST and NDVI) were extracted for the study periods. The number and location of the values were selected in such a way as to capture as many healthy mangrove vegetation states as possible with their corresponding surface temperatures.

2.6 Local Bivariate Analysis for LST-NDVI relationship determination

LBA was conducted to determine statistically significant relationships between LST and NDVI for the region of interest by using local entropy. The relationships between LST and NDVI were presented in six classes: Positive Linear, Negative Linear, Concave, Convex, Unidentified Complex and Not Significant. The output of LBA was used to visualize the areas where the LST-NDVI was related and how their association varied over the study region. To accomplish this, point feature containing LST and NDVI data for each of the considered years was introduced as the input feature. Then, NDVI was assigned as the depended variable and LST was introduced to be the explanatory variable. The number of neighbours around the feature that was used to identify local relationships between the two variables was kept at 30 (i.e., the default value). This value had the sufficient magnitude to derive a relationship between LST and NDVI for the mangroves. Also, this value managed to identify local variations in pattern for the relationship. The number of permutations was set at the default value of 199. This value was used to compute pseudo p-value for the variables. With this specific number, the smallest pseudo p-value was 0.005 and all the other pseudo p-values were the multiples of this smallest pseudo p-value. Finally, the level of confidence was set at 90% of the hypothesis test for significant relationships.

3. Results and Discussion

Figure 3 shows how LST-NDVI relationship was locally varied throughout the study site for the year 2015 and 2020 based on the sample points through which LST and NDVI values were previously extracted from. The mangrove area was segmented into two zones (i.e., 1 and 2) in both cases.

From Figure 3a, it is discerned that zone 1 mostly exhibited positively linear and Concave relationships between LST and NDVI with some non-significant associations at the north-western, north-eastern and south eastern sides. Positively Linear relationship indicated that as LST values increased, the corresponding NDVI values also increased. Whereas, Concave relationship referred to the increase in mangrove NDVI with LST till the vegetation health state reached a certain maximum value. Then, further increase in temperature degraded the health condition. Zone 2 showcased quite a different type of LST-NDVI relationship from zone 1 for the major area. Firstly, it covered Negatively Linear relationship for more than 50% of the covered area, indicating that increase in LST caused decrease in mangrove NDVI. However, for the south-eastern portion of the zone, it showed the same Concave relationship that was found in Zone 1.

From Figure 3b, zone 1 showed mostly Negative Linear LST-NDVI association, with a bit of Concave distribution at the northern side. Whereas, there were few points depicting Not Significant LST-NDVI relationships, prevailing at the southern side of the zone. Zone 2 was governed by two types of LST-NDVI relationships. Those were Convex and Negative Linear. Convex relationship meant the fall of mangrove vegetation health with increase in surface temperature up to a certain minimum value. Then, further increase in temperature increased mangrove health index.

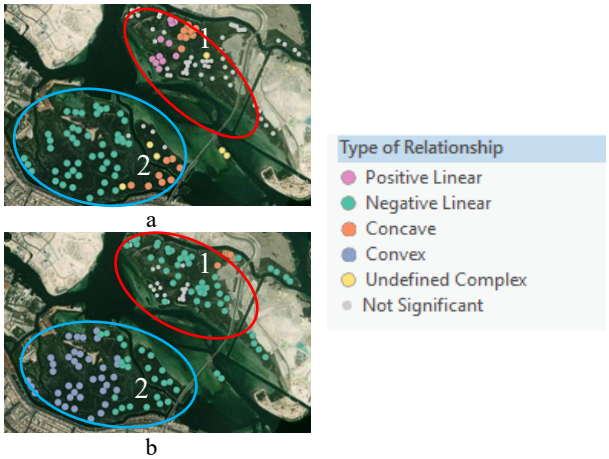

Figure 3. LBA to determine LST-NDVI relationship types for the year (a) 2015 and (b) 2020; Zone 1 circled in red and Zone 2 circled in blue

To further elaborate on the local LST-NDVI relationship variations, scatterplots were generated for the study area, covering each year which showcased in detail how and to which extent LST influenced mangrove NDVI for a specific portion of the study region for a given year. Under this situation, relationship types falling under Unidentified Complex and Not Significant were ignored. Since these correlations could not yield any kind of graphs for further analysis and explanations. The graphs containing both explanatory variable (i.e., LST) and dependent variable (i.e., NDVI) were rescaled to fit within the range 0-1 (this was accomplished by subtracting the minimum value of the dataset from each value and further dividing it by the difference between the maximum and the minimum value of the dataset for each variable) (Figure 4, Figure 5).

From Figure 4a, it is observed that lowest temperature of 0.35 corresponded to the highest NDVI of 0.76. As temperature started to rise, there was a linear fall of NDVI with the minimum value reached was 0.36, corresponding to the maximum LST of 0.80 unit. Figure 4b showed a Concave trend between LST and NDVI for the mangrove at Abu Dhabi. 0.25 unit of LST provided around 0.11 unit of NDVI. As LST started to increase, so did NDVI. At LST of 0.47 unit, NDVI reached its highest peak, with approximately 0.60 unit. Beyond this LST value, mangrove NDVI started to decrease. Figure 4c showed a positive linear trend between LST and NDVI. With minimum LST of 0.25 caused the NDVI to be around 0.35. Further increase in LST made NDVI to rise as well.

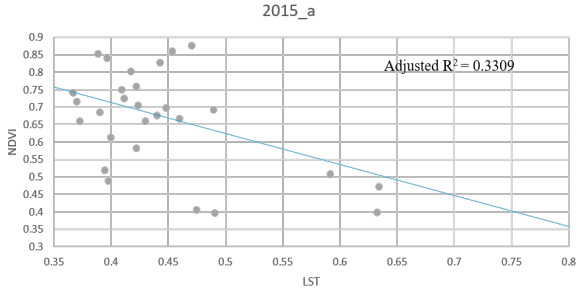

a

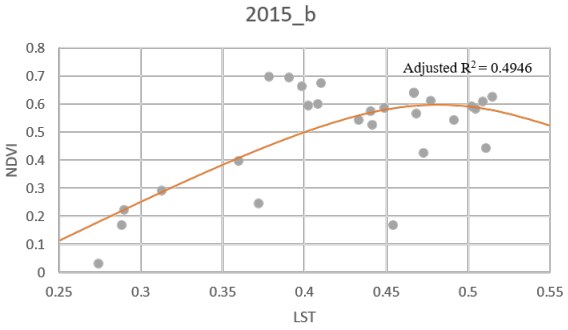

b

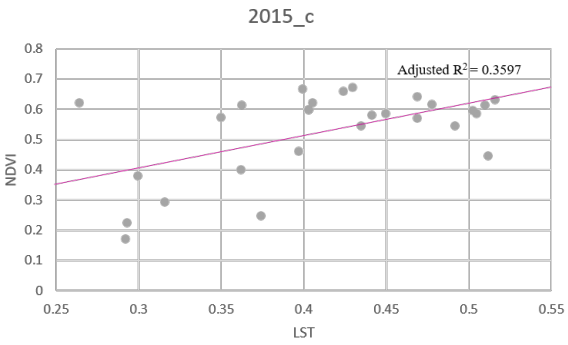

c

Figure 4. Scatterplots depicting a. Negative Linear (Zone 2), b. Concave (Zone 1 and 2), c. Positive Linear (Zone 1) LST-NDVI relationships for Abu Dhabi mangrove considering the year 2015

For 2020, Figure 5a demonstrated a negatively decreasing (i.e. convex) trend between LST and NDVI for the mangrove. As temperature reached 0.35 unit, the corresponding NDVI fell to the minimum value of about 0.30 unit. Figure 5b showed negative linear influence of LST on NDVI. Where a low LST of 0.07 was depicted to provide high NDVI value of over 0.82. As LST started to increase, mangrove vegetation health state fell linearly. From Figure 5c, it could be observed that a low LST of 0.10 unit caused peak mangrove NDVI at around 0.71. As temperature started to increase, there was increasing fall of mangrove health condition. When LST was found to be at 0.38 unit, mangrove NDVI decreased to at around 0.33.

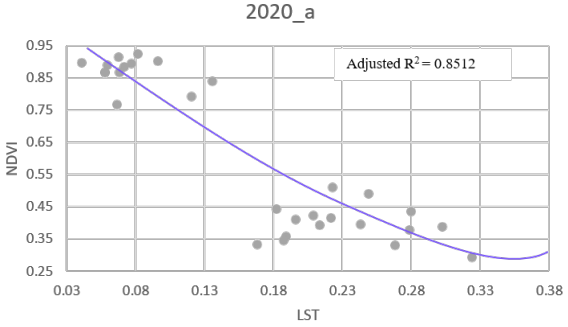

a

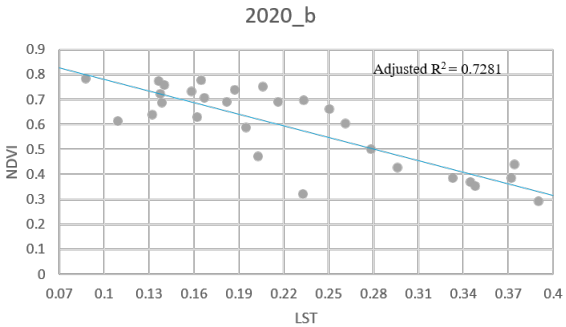

b

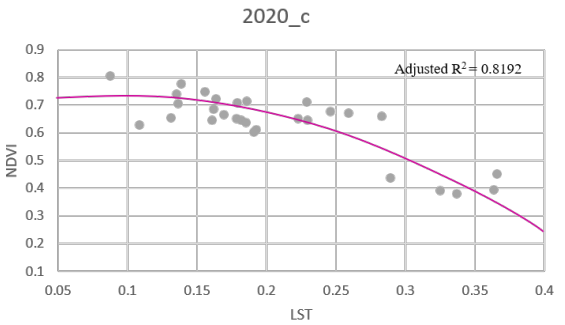

c

Figure 5. Scatterplots depicting a. Convex (Zone 2), b. Negative Linear (Zone 1 and 2), c. Concave (Zone 1) LST-NDVI relationships for Abu Dhabi mangrove considering the year 2020

By observing all the LST-NDVI relationship patterns for the years 2015 and 2020, it could be postulated that the influence of LST on mangrove NDVI was complex as not a single type of association chiefly governed between the two environmental parameters. So far, focus was given to understand the effect of mangrove vegetation health on surface temperature (Kanjin & Alam, 2024), (Rostami et al., 2022), (Ruan et al., 2022). But this study attempted at deriving the localized impacts of LST on NDVI for mangrove in Abu Dhabi, UAE. General observation from the plots (Figure 4a, Figure 5a, Figure 5b, and Figure 5c) dictated that increase in LST caused decrease in NDVI in major portions of the study area for both the years and this phenomenon was supported by previously published literature(s) (Cobacho et al., 2024), (Lovelock et al., 2016). For this specific research, LST-NDVI relationships were diverse in nature when different zones of a chosen region of interest (i.e., Abu Dhabi Mangrove National Park) were considered over a certain timeframe (i.e., between years 2015 and 2020). Whereas, globally conducted previous studies either covered the detrimental effects on mangrove vegetation due to high temperature (Cobacho et al., 2024), (Rendana et al., 2023) or substantially low temperatures (Chen et al., 2017), (Osland et al., 2017), (Lovelock et al., 2016). Furthermore, coefficient of determinations for the LBA trends obtained for 2020 were much higher compared to that of 2015 with the highest $R^2 = 0.8512$ (portraying Convex relationship) followed by $R^2 = 0.8192$ (Concave) and $R^2 = 0.7281$ (Negative Linear). This study could be further improved by conducting LBA on more mangrove sites in UAE for larger time durations to determine the most assertive LST-NDVI relationship(s).

This contribution has been peer-reviewed. The double-blind peer-review was conducted on the basis of the full paper.
https://doi.org/10.5194/isprs-annals-X-G-2025-681-2025 | © Author(s) 2025. CC BY 4.0 License.

4. Conclusion

The impact of microclimate (i.e., LST) on mangrove health (i.e., NDVI) was shown to be quite spatially and temporally varied across the coastal area of Abu Dhabi, UAE. The variance encompassed Positive Linear, Negative Linear, Concave, Convex, and Not Significant relationships based on the point features used to extract LST and NDVI data from Landsat 8 satellite imageries. Additionally, overall inspection of the scatterplots revealed that LST caused mangrove health to deteriorate for both 2015 and 2020. Moreover, the later year provided higher R^2 values for the LST-NDVI models. The findings of this study could potentially help in formulating government/non-government policies towards mangrove conservation.

Acknowledgements

The authors would like to acknowledge the support received from FRG21-M-E77 (American University of Sharjah).

References

Akbar, M. R., Arisanto, P. A. A., Sukirno, B. A., Merdeka, P. H., Priadhi, M. M., & Zallesa, S., 2020. Mangrove vegetation health index analysis by implementing NDVI (normalized difference vegetation index) classification method on sentinel-2 image data case study: Segara Anakan, Kabupaten Cilacap. *IOP Conference Series: Earth and Environmental Science*, *584*(1). https://doi.org/10.1088/1755-1315/584/1/012069

Alongi, D. M., 2015. The Impact of Climate Change on Mangrove Forests. *Current Climate Change Reports*, *1*(1), 30–39. https://doi.org/10.1007/s40641-015-0002-x

Bashitialshaaer, R. A. I., Persson, K. M., & Aljaradin, M. (2011). Estimated future salinity in the Arabian Gulf, the Mediterranean Sea and the Red Sea consequences of brine discharge from desalination. *International Journal of Academic Research*, *3*(1).

Chen, L., Wang, W., Li, Q. Q., Zhang, Y., Yang, S., Osland, M. J., Huang, J., & Peng, C., 2017. Mangrove species' responses to winter air temperature extremes in China. *Ecosphere*, *8*(6), 1–14. https://doi.org/10.1002/ecs2.1865

Cobacho, S. P., Janssen, S. A. R., Brekelmans, M. A. C. P., van de Leemput, I. A., Holmgren, M., & Christianen, M. J. A., 2024. High temperature and eutrophication alter biomass allocation of black mangrove (Avicennia germinans L.) seedlings. *Marine Environmental Research*, *193*(November 2023), 106291. https://doi.org/10.1016/j.marenvres.2023.106291

Kanjin, K., & Alam, B. M., 2024. Assessing changes in land cover, NDVI, and LST in the Sundarbans mangrove forest in Bangladesh and India: A GIS and remote sensing approach. *Remote Sensing Applications: Society and Environment*, *36*(February), 101289. https://doi.org/10.1016/j.rsase.2024.101289

Liu, X., Liu, H., Chen, L., & Wang, X., 2022. Ecological interception effect of mangroves on microplastics. *Journal of Hazardous Materials*, *423*, 127231.

Lovelock, C. E., Krauss, K. W., Osland, M. J., Reef, R., & Ball, M. C., 2016. The Physiology of Mangrove Trees with Changing Climate. *Tropical Tree Physiology*, 149–179. https://doi.org/10.1007/978-3-319-27422-5

Malik, A., Mertz, O., & Fensholt, R., 2017. Mangrove forest decline: consequences for livelihoods and environment in South Sulawesi. *Regional Environmental Change TA - TT -*, *17*(1), 157–169. https://doi.org/10.1007/s10113-016-0989-0 LK - https://aus.on.worldcat.org/oclc/6947860093

Moore, G. E., Grizzle, R. E., & Ward, K. M., 2013. *Mangrove resources of the United Arab Emirates: mapping and site survey 2011–2013*. Final Report to the United Arab Emirates Ministry of Environment and Water, University of New Hampshire, Jackson Estuarine Laboratory, Durham, NC, USA.

Morris, J. T., Langley, J. A., Vervaeke, W. C., Dix, N., Feller, I. C., Marcum, P., & Chapman, S. K., 2023. Mangrove Trees Outperform Saltmarsh Grasses in Building Elevation but Collapse Rapidly Under High Rates of Sea-Level Rise. *Earth's Future*, *11*(4). https://doi.org/10.1029/2022EF003202

Muhsoni, F. F., Sambah, A. B., Mahmudi, M., & Wiadnya, D. G. R., 2018. Comparison of different vegetation indices for assessing mangrove density using sentinel-2 imagery. *International Journal of GEOMATE*, *14*(45), 42–51. https://doi.org/10.21660/2018.45.7177

Osland, M. J., Day, R. H., Hall, C. T., Brumfield, M. D., Dugas, J. L., & Jones, W. R., 2017. Mangrove expansion and contraction at a poleward range limit: Climate extremes and land-ocean temperature gradients. *Ecology*, *98*(1), 125–137. https://doi.org/10.1002/ecy.1625

Osland, M. J., Hartmann, A. M., Day, R. H., Ross, M. S., Hall, C. T., Feher, L. C., & Vervaeke, W. C., 2019. Microclimate Influences Mangrove Freeze Damage: Implications for Range Expansion in Response to Changing Macroclimate. *Estuaries and Coasts*, *42*(4), 1084–1096. https://doi.org/10.1007/s12237-019-00533-1

Parks, S., 2020. *The importance of calibrating your remote sensing imagery*. Malvern Panalytical. https://www.malvernpanalytical.com/en/learn/knowledge-center/insights/the-importance-of-calibrating-your-remote-sensing-imagery#:~:text=Radiometric calibration%2C also known as,objects on the ground's surface (23 January 2025).

Raihan, A., Ali, T., & Mortula, M., 2024. Unveiling coastal ecosystem dependencies: multifactorial analysis of climate change influencing mangrove system in the United Arab Emirates over the period 1990–2020. *Discover Sustainability*, *5*(1). https://doi.org/10.1007/s43621-024-00620-9

Raihan, A., Ali, T., Mortula, M., & Gawai, R., 2023. Spatiotemporal Analysis of the Impacts of Climate Change on Mangroves Located in the United Arab Emirates. *Journal of Sustainable Development of Energy, Water and Environment Systems*, *11*(3), 1–19. https://doi.org/https://doi.org/10.13044/j.sdewes.d11.0460

Rendana, M., Razi Idris, W. M., Abdul Rahim, S., Ghassan Abdo, H., Almohamad, H., Abdullah Al Dughairi, A., & Albanai, J. A., 2023. Effects of the built-up index and land surface temperature on the mangrove area change along the southern Sumatra coast. *Forest Science and Technology*, *19*(3), 179–189. https://doi.org/10.1080/21580103.2023.2220576

Rostami, F., Attarod, P., Keshtkar, H., & Tahroudi, M. N., 2022.

Impact of climatic parameters on the extent of mangrove forests of southern Iran. *Caspian Journal of Environmental Sciences*, *20*(4), 671–682. https://doi.org/10.22124/cjes.2022.5719

Ruan, L., Yan, M., Zhang, L., Fan, X., & Yang, H., 2022. Spatial-temporal NDVI pattern of global mangroves: A growing trend during 2000–2018. *Science of The Total Environment*, *844*, 157075.
https://doi.org/https://doi.org/10.1016/j.scitotenv.2022.157075

Siddan., A., & C.R., P., 2016. Statistical Correlation between Land Surface Temperature (LST) and Vegetation Index (NDVI) using Multi-Temporal Landsat TM Data. *International Journal of Advanced Earth Science and Engineering*, *5*(1), 333–346. https://doi.org/10.23953/cloud.ijaese.204

Sam, S. C., & Balasubramanian, G., 2023. Spatiotemporal detection of land use/land cover changes and land surface temperature using Landsat and MODIS data across the coastal Kanyakumari district, India. *Geodesy and Geodynamics*, *14*(2), 172–181. https://doi.org/10.1016/j.geog.2022.09.002

Shawky, M., Ahmed, M. R., Ghaderpour, E., Gupta, A., Achari, G., Dewan, A., & Hassan, Q. K., 2023. Remote sensing-derived land surface temperature trends over South Asia. *Ecological Informatics*, *74*(November 2022), 101969. https://doi.org/10.1016/j.ecoinf.2022.101969

Simard, M., Fatoyinbo, L., Smetanka, C., Rivera-Monroy, V. H., Castañeda-Moya, E., Thomas, N., & Van der Stocken, T., 2019. Mangrove canopy height globally related to precipitation, temperature and cyclone frequency. *Nature Geoscience*, *12*(1), 40–45. https://doi.org/10.1038/s41561-018-0279-1

T.S., A., 2014. An assessment of Avicennia Marina forest structure and aboveground biomass in eastern mangrove lagoon national Park, Abu Dhabi LK - https://aus.on.worldcat.org/oclc/8088133934. *Arab World Geographer TA - TT* -, *17*(2), 166–185.

USGS Earth Explorer. https://earthexplorer.usgs.gov/ (May 15, 2022)

Wu, Y., Ricklefs, R. E., Huang, Z., Zan, Q., & Yu, S., 2018. Winter temperature structures mangrove species distributions and assemblage composition in China. *Global Ecology and Biogeography*, *27*(12), 1492–1506. https://doi.org/10.1111/geb.12826

Xu, H. Q., & Huang, S. L., 2016. A Comparative Study on the Calibration Accuracy of Landsat 8 Thermal Infrared Sensor Data. *Guang Pu Xue Yu Guang Pu Fen Xi= Guang Pu*, *36*(6), 1941–1948.